The dynamics of deepwater offloading buoys

A. Duggal & S. Ryu
Research & Development Department,
FMC SOFEC Floating Systems, Inc., USA.

Abstract

Deepwater offloading buoys are being used in West Africa to allow efficient loading of spread-moored FPSOs. These buoys have a relatively small displacement when compared to other floating systems, with the majority of the displacement being used to support the mooring system and the oil offloading lines. This results in a floating system that has a very active response to the environment, coupled with feedback from the mooring and flowline systems. This wave frequency dominant motion behaviour has been shown to result in severe fatigue damage to the mooring and flowline components, and thus must be estimated accurately to ensure that the system is designed with sufficient fatigue life.

The paper presents results from time- and frequency-domain simulations of the offloading buoy system to demonstrate its response characteristics. The results and comparisons demonstrate the importance of accounting for the coupling between the mooring and flowline system, and the buoy hull in predicting the system response. Results from sensitivity studies are also be presented to show the relative importance of the mooring and flowline system mass, stiffness and damping contributions to the system response, and thus the fatigue life of the various components. The response of the buoy with an offloading tanker connected is also be presented and compared to that of the buoy alone.

Keywords: fluid-structure interaction, coupled analysis, offloading buoy, FPSO, floating platform.

1 Introduction

Deepwater offloading buoys are being utilized in West Africa to provide large, spread-moored FPSOs with the desired offloading operability. These offloading

buoys are typically located one nautical mile from the vessel. Two or three large flowlines (typically flexible or steel pipe) run in a suspended catenary between the FPSO and the offloading buoy. These flowlines exert large loads on the buoy that need to be reacted by the buoy's displacement and mooring system. Typical mooring systems are constructed of chain and polyester rope or spiral strand wire with a total of seven to ten anchor legs. The typical water depth for such systems is 1,000 to 2,000 meters. Figure 1 illustrates a deepwater offloading buoy with a tanker moored to it.

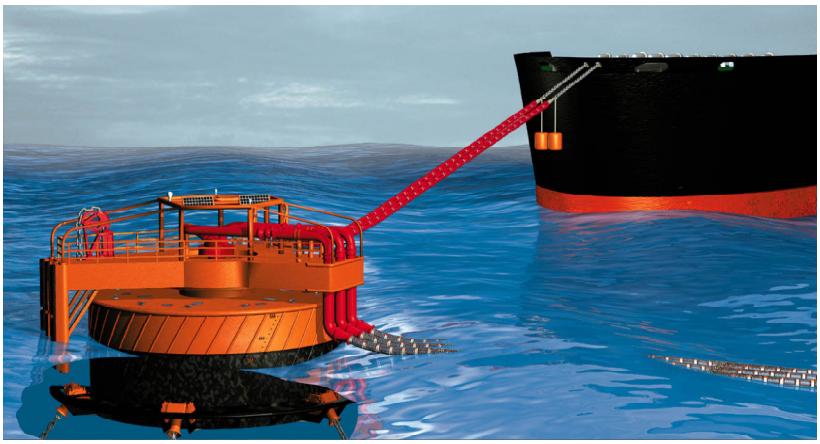

Figure 1: Offloading from a deepwater offloading buoy.

A typical offloading buoy has a diameter of approximately 25 meters and a draft of 5 to 6 meters with a moored displacement of approximately 2,500 MT. Typical heave, roll and pitch natural periods are around 7 to 10 seconds, resulting in a buoy that has a very active response to the environment. The mooring system for the buoy is designed to counteract the large horizontal forces from the flowlines (approximately 250 to 300 MT), and to provide stationkeeping for the buoy during offloading. Thus the mooring system is asymmetric with very different stiffness as a function of direction, resulting in coupling between different modes of motion, e.g., surge and yaw. In addition the mooring and flowline stiffness have a significant effect on the motions of the buoy due to the comparable mass, large stiffness and viscous interaction with the fluid. This complex interaction between the various components is further complicated when a tanker is connected to the buoy with a hawser.

It has been well documented from experience and past work [1, 2] that these buoys have a very active and complex response and that care must be taken to properly estimate the motions of the buoy and its impact on the response (and fatigue life) of the anchor legs and flowlines. This is underscored by the failure of four anchor legs on the Girassol offloading buoy within a year of installation. These legs failed due to fatigue of the chain at the interface with the buoy,

caused by the excessive motions of the buoy system that resulted in chain bending [3].

The objective of this paper is to provide a description of the methodology and numerical methods used by the authors to estimate the response of the offloading buoy, both alone and when offloading to a tanker of opportunity. The response characteristics obtained from this methodology are presented along with a brief parametric study of the influence of the viscous forces on components of the system.

2 Modelling of the coupled system

As described above the buoy offloading system has high complexity due to the multi-object coupling among the buoy, mooring system, flowlines (OOLs) and the tanker. To accurately capture the waves and current loading on each object, it is necessary to identify and implement the effect of both inertia and viscous loading on each component of the buoy system. To accomplish this we utilize a fully-coupled time-domain numerical model that uses a diffraction model of the buoy, with additional drag elements to model the buoy hull and the skirt to capture viscous effects. In addition all flowlines and mooring lines are modelled using finite elements where the fluid loading is represented by Morison's equation. The complete equations of motion are solved using DeepLines, a fully-coupled time-domain analysis program [4]. DeepLines also allows for the complete representation of the non-linear hawser stiffness and the offloading tanker to provide a complete, time-domain description of the offloading system response. Figure 2 provides a screen-capture of the numerical model that shows the components of the system modelled. The FPSO end of the flowlines is excited by the FPSO RAOs as the low-frequency responses of the FPSO have been shown to not strongly influence the response of the offloading buoy due to the low stiffness of the flowlines.

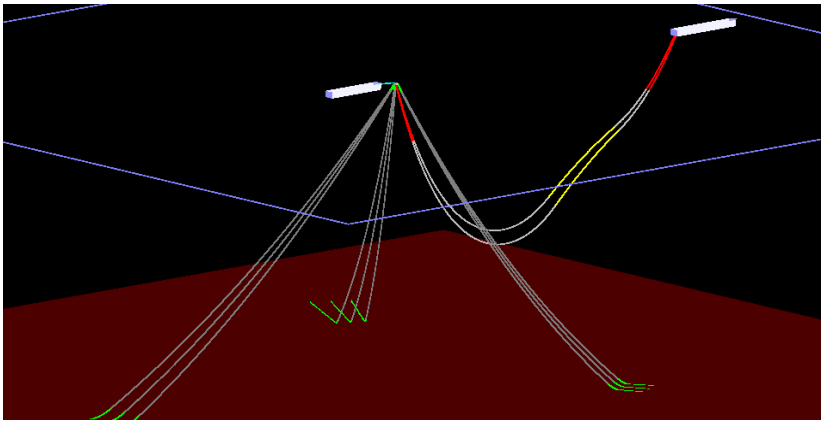

Figure 2: Screen capture of offloading buoy system modelled in DeepLines.

2.1 Numerical model of buoy

As an example a hypothetical buoy in 1,400 meters water depth, offshore West Africa is modelled. The buoy is 23 meters in diameter and has a draft of 5.8 meters. The mooring system has nine anchor legs made of chain and spiral strand wire, and two steel flowlines connecting the buoy to the FPSO.

The diffraction analysis of the buoy hull has been performed using a higher order boundary element method program HOBEM. HOBEM is used to evaluate added mass, radiation damping, and the linear wave loads [5, 6]. The skirt is included in the mesh generation to take into account its effect on the added mass and radiation damping. The holes in the skirt and the centerwell were not meshed to eliminate numerical instability issues. However, the 6×6 inertia matrix of the buoy hull is modified to account influence for the centerwell.

Not only does the buoy skirt affect the added mass and radiation damping, but it also generates either viscous damping and/or drag force depending on its relative velocity to the wave kinematics in the surrounding velocity field. To take into account viscous/drag effects caused by a skirt, Morison type drag elements are implemented by using multiple disks as shown in Figure 3. Since the skirt-induced added mass and inertia force are already taken into account in the radiation/diffraction problem, the inertia coefficient of the disks was set to zero. The detailed viscous/drag modelling in each 6-DOF direction is summarized in Table 1. Additional details on the modelling of the buoy are suggested by Ryu *et al* [7].

Figure 4 presents a summary of the wave exciting forces on the buoy system computed for a representative environment for the West of Africa, using the results from the buoy hull model.

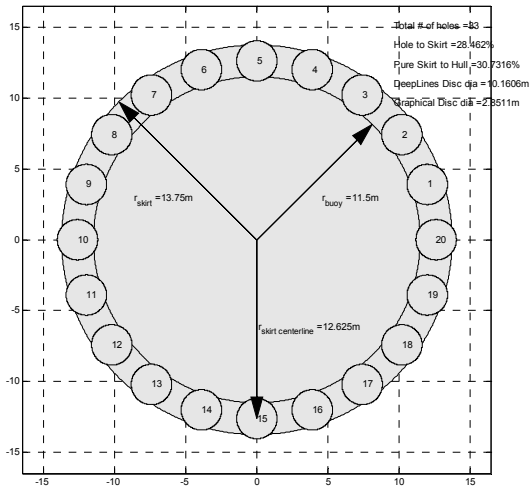

Figure 3: Skirt modelling by using multiple disks.

Table 1: Summary of buoy viscous/drag modelling.

		Velocity Used		Linear or Quadratic		Cd or D
Mode		Absolute	Relative	Linear	Quadratic	
Surge			√		√	2.0
Sway			√		√	2.0
Heave		√	√	√	√	5.29e5 & 4.5
Roll	Hull	√			√	6.152e9
	Skirt		√		√	6.0
Pitch	Hull	√			√	6.152e9
	Skirt		√		√	6.0
Yaw		√			√	1.202e8

The mooring system and flowlines are modelled using finite elements within the program DeepLines with complete representation of mass and stiffness. The fluid interaction is modelled using the relative motion form of Morison's equation. For the offloading cases nonlinear hawser stiffness is used to represent the characteristics of the nylon rope construction. The offloading tanker is represented by a model incorporating both the first- and second-order forces from a program like HOBEM.

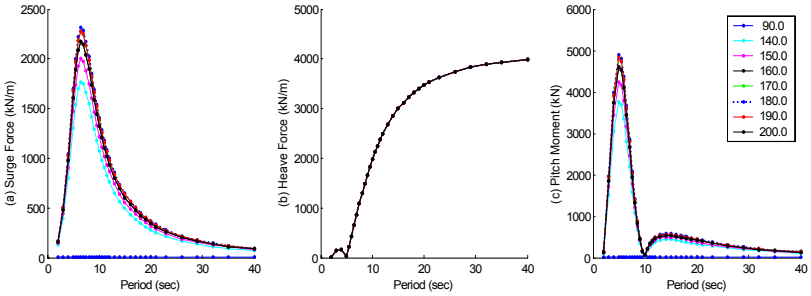

Figure 4: For eight different wave incident angles, first order wave exciting force/moment in (a) surge, (b) heave and (c) pitch directions.

The numerical model described briefly above has been validated against an experimental data set from a model test program conducted in 1999 [8]. Details of the validation are presented in [7]. A comparison of the free decay tests are presented here to illustrate the accuracy of the model in predicting the buoy response in controlled conditions. Surge, heave and pitch free decay experimental data and numerical calculations are compared and shown in Figure 5. The comparison shows that the numerical model properly represents the buoy response and damping over a wide range of amplitudes, illustrating its accuracy.

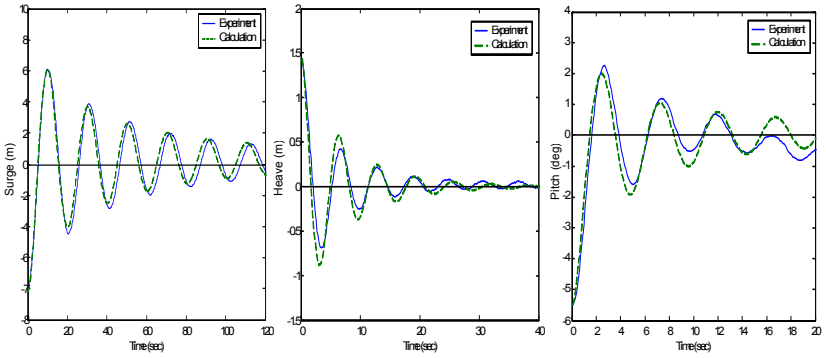

Figure 5: Surge (left), heave (centre), and pitch (right) and free decay tests for the moored case: solid line - experiment, dashed line – calculation.

3 Calculation results: buoy motion RAOs

The analysis is performed in DeepLines with both regular and irregular waves to generate estimates of buoy response. RAOs as a function of wave incidence have been generated for both the buoy alone case as well as for the case with a 315kDWT offloading tanker moored to the buoy using a nylon hawser. In addition a small parametric study of buoy response (alone) has been performed to study the influence of viscous forces by modifying the drag coefficient on various components.

The coordinate system shown in Figure 6 is used in the analysis. The incident angle of 180 degrees represents the case of seas and swell coming from positive X-axis, which is in-line to the flowlines.

3.1 Buoy alone case

The motion RAOs of the buoy were derived at the buoy centre of gravity for three different wave incident angles. Figures 7 through 9 present RAOs for all six degrees of freedom of the buoy over a wide range of periods.

The results illustrate the influence of the mooring and flowline system on the buoy response. Differences in the surge and sway response as a function of wave heading illustrate the influence of the asymmetric nature of the mooring stiffness. This is also illustrated in the yaw RAO that clearly shows that as the angle of incidence deviates from the axis of symmetry of the buoy that there is a stronger yaw response of the buoy. This is caused primarily by the asymmetric stiffness and the increasing sway motion where the balance of forces from the mooring and the flowlines causes the buoy to rotate. Further complicating this response is that the natural period of yaw for this example is around 10 seconds and thus the yaw response is subject to dynamic amplification. This is one mode of vibration of the system that can lead to rapid fatigue of the chain and flowlines at their attachment points to the buoy.

The roll and pitch RAOs are also seen to have two sharp peaks. Parametric studies have shown that the double peak is caused by the skirt and the depth of the valley is a function of the damping/drag generated by the skirt and the hull. This is shown in Figure 10 that summarizes results from a parametric study.

Figure 11 presents the buoy response as a function of viscous forces on the mooring system by varying Cd between 0.6 and 2.0. The figure shows that the influence on buoy response is limited to the heave response at the natural period, and the pitch response at longer wave periods.

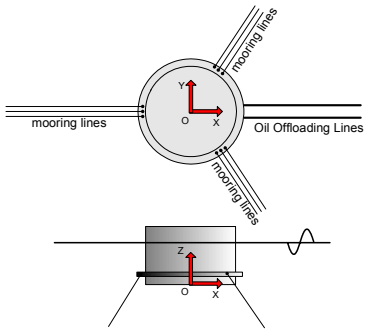

Figure 6: Buoy local coordinate system.

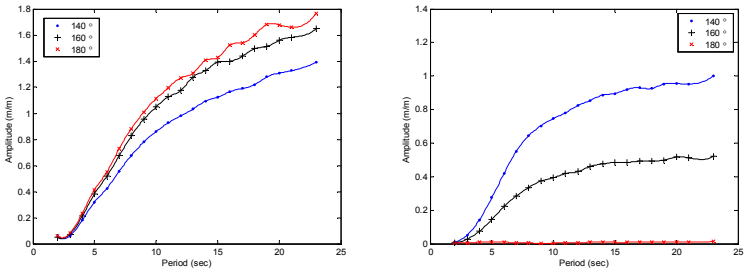

Figure 7: Surge (left) and sway (right) RAOs for three incident wave angles.

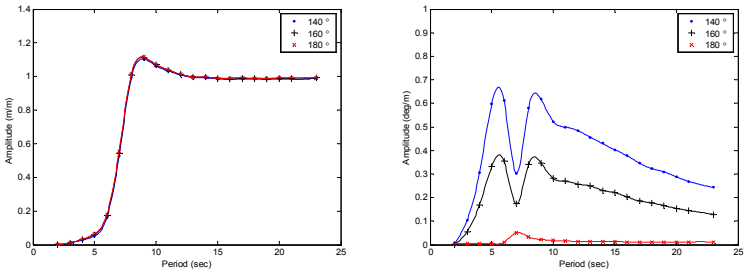

Figure 8: Heave (left) and roll (right) RAOs for three incident wave angles.

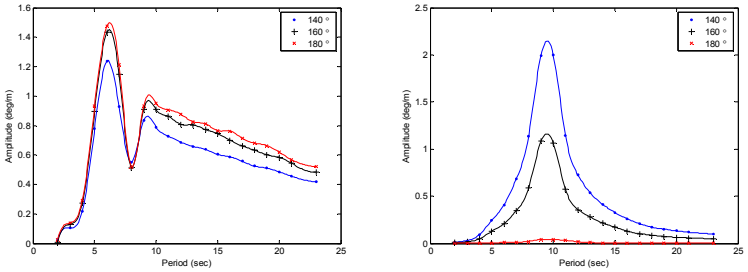

Figure 9: Pitch (left) and yaw (right) RAOs for three incident wave angles.

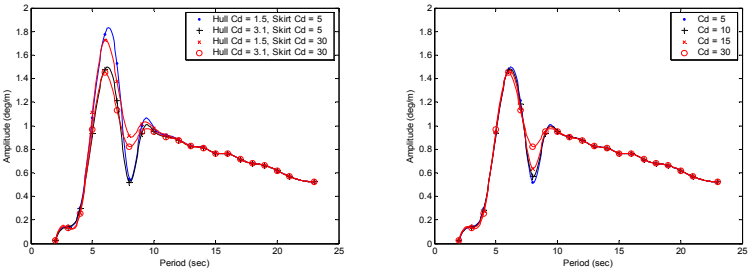

Figure 10: Sensitivity of the buoy hull damping vs. skirt viscous damping (left) and of the buoy skirt viscous damping (right).

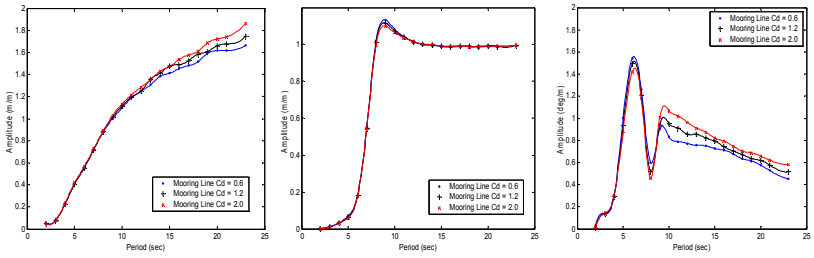

(a) (b) (c)

Figure 11: Sensitivity of the mooring line Cd: (a) surge, (b) heave, and (c) pitch RAOs; dot(.) – Cd = 0.6, plus(+) – Cd = 1.2, cross(x) – Cd = 2.0.

3.2 Buoy with tanker connected case

Figures 12 through 14 present the buoy motion RAOs influenced by the tanker moored with a nylon hawser. The mean load in the hawser and its stiffness results in an increase in the inline stiffness of the buoy system and causes significant change in the surge, sway, roll and pitch RAOs as shown in the figures, especially between 15 and 25 seconds. The yaw and heave RAOs are relatively unchanged. This modification of response, commonly neglected in engineering design, can have a very significant impact on the fatigue life of the

mooring and flowline components as for large FPSOs the buoy can spend 25% of the time with a tanker moored to it.

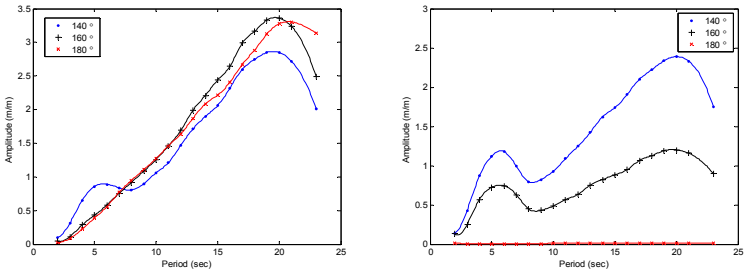

Figure 12: Surge (left) and sway (right) RAOs for three incident wave angles.

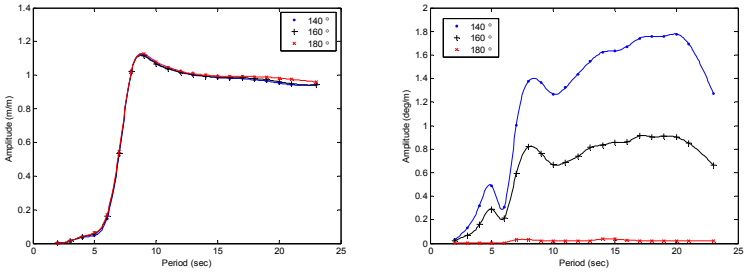

Figure 13: Heave (left) and roll (right) RAOs for three incident wave angles.

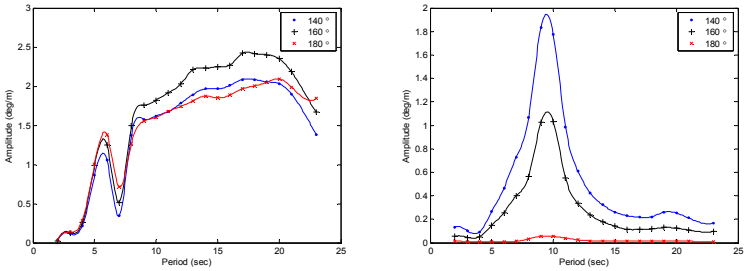

Figure 14: Pitch (left) and yaw (right) RAOs for three incident wave angles.

4 Summary and conclusions

The paper presents the results of a numerical model that illustrates the complex response of deep water offloading buoys, currently used to enhance the offloading performance of spread-moored FPSOs, offshore West Africa. The paper presents an overview of the methodology and model used to represent the buoy system, with an emphasis on representing both the inertial and viscous

forces on the buoy and its mooring and flowline systems. Buoy response estimates were presented in the form of RAOs for all six degrees of freedom for both the buoy alone, and with a VLCC tanker moored with a nylon hawser.

The results showed the influence of the mooring system and the viscous forces on the response of the buoy. The paper also showed the modification of the buoy response with a tanker moored that is commonly overlooked in engineering analysis and design of such a system and can have a marked impact on the fatigue life estimate of the mooring and flowline system of the buoy.

References

[1] Levi, C.F., Teixeira, M. & Aratanha, M., Monobuoys for deep water. *Proc. of OMAE*, OMAE, St. John's, Canada, 1999.

[2] Heyl, C.N., Zimmermann, C., Eddy, S.L. & Duggal, A.S., Dynamics of suspended mid-water flowlines. *Proc. of OMAE*, OMAE, Rio De Janeiro, Brazil, 2001.

[3] Jean, P., Goessens, K. & L'Hostis, D., Failure of chains by bending in deepwater mooring systems. *Proc. of Offshore Technology Conference*, OTC 17238, Houston, USA, 2005.

[4] *DeepLines Theory Manual*, V4.1, Principia RD & IFP, 2004.

[5] Liu, Y.H., Analysis of fluid-structure interaction by using higher-order boundary elements in potential problems and its application in coupling vibrations of bending and torsion of ships, Ph.D. Dissertation, Shanghai Jiao Tong University, China, 1988.

[6] Liu, Y.H., Kim, C.H. & Lu, X.S., Comparison of higher order boundary element and constant panel method for hydrodynamic loading. *Int. J. Offshore and Polar Engineering*, **1(1)**, pp. 8-17, 1991.

[7] Ryu, S., Duggal, A.S., Heyl, C.N. & Liu, Y., Coupled analysis of deepwater oil offloading buoy and experimental verification. *Proc. of the Fifteenth Int. Offshore & Polar Engineering Conference*, Seoul, Korea, pp. 148-155, 2005.

[8] Colbourne, D.B., Deep water CALM buoy moorings wave basin model tests. *Technical Report*, Institute for Marine Dynamics, National Research Council Canada, TR-2000-06, 2000.